REPORT

POLYMERS

Combining polyethylene and polypropylene: Enhanced performance with PE/*i*PP multiblock polymers

James M. Eagan,[1] Jun Xu,[2] Rocco Di Girolamo,[1]* Christopher M. Thurber,[2] Christopher W. Macosko,[2] Anne M. LaPointe,[1]† Frank S. Bates,[2]† Geoffrey W. Coates[1]†

Polyethylene (PE) and isotactic polypropylene (*i*PP) constitute nearly two-thirds of the world's plastic. Despite their similar hydrocarbon makeup, the polymers are immiscible with one another. Thus, common grades of PE and *i*PP do not adhere or blend, creating challenges for recycling these materials. We synthesized PE/*i*PP multiblock copolymers using an isoselective alkene polymerization initiator. These polymers can weld common grades of commercial PE and *i*PP together, depending on the molecular weights and architecture of the block copolymers. Interfacial compatibilization of phase-separated PE and *i*PP with tetrablock copolymers enables morphological control, transforming brittle materials into mechanically tough blends.

Polyethylene (PE) and isotactic polypropylene (*i*PP) are the two most abundantly produced plastics worldwide. More than 70 million and 50 million metric tons of PE and *i*PP, respectively, are produced annually (*1*). The vast majority of PE and *i*PP are prepared using heterogeneous chromium and titanium catalysts (*2*). Heterogeneous olefin polymerization catalysts have a multitude of active sites, each with their own reactivity differences that give rise to polymers of different molecular weights (MW), MW distributions, and microstructures (*3*). In the case of PE and *i*PP, these differences and their phase separation inhibit interfacial adhesion and erode the mechanical properties of melt blends (*4*). Roughly 5% of the value is retained when these plastics are recycled, typically into lower-value products as a result of sorting expenses and degraded physical properties (*5*). Compatibilizers open opportunities for upcycling recovered PE/*i*PP into equal- or higher-value materials with lower sorting costs (*6*, *7*). Because PE and *i*PP are of great economic importance (more than ~$200 billion in annual sales, worldwide), strategies to combine these materials may have considerable potential to affect sustainability and the economy.

Single-site metallocene catalysts have been developed and commercialized to produce polyolefins with a more uniform molecular composition (*8*). These polymers demonstrate distinct physical properties from their heterogeneous counterparts, such as the ability to form interfacial welds (*9*). Many nonmetallocene single-site catalysts have also been developed, some of which demonstrate living character for olefin polymerization as well as precise control over the MW, stereochemistry, and architecture of the resulting polymer (*10*, *11*).

Strategies to compatibilize *i*PP and PE rely on the addition of large amounts (≥10%) of additives, typically amorphous polymers (*12*–*14*). We became interested in how block copolymers of PE and *i*PP would behave as additives in commercial heterogeneous-grade polyolefin materials. Despite the simplicity of this idea, we are aware of only a single example of a well-defined semicrystalline polymer combining blocks of PE and *i*PP. Busico and co-workers used a modified C_2-symmetric zirconium catalyst to synthesize a PE-*b*-*i*PP diblock copolymer (*15*, *16*). The *i*PP block was shown to be unusually stereoregular [*mmmm* pentad content (*8*) (m^4) = 99%; melting temperature (T_m) = 152°C] and polymerization was well controlled [dispersity ($Đ$) = 1.3], but number-average MWs were relatively low (M_n = 22 kg/mol) (*16*). Experimental results revealed that the catalyst underwent β-hydride elimination, resulting in limited chain growth and accessible architectures. As part of our long-standing interest in living olefin polymerization, we sought to develop improved catalysts with longer lifetimes capable of producing higher-MW PE/*i*PP diblock and multiblock copolymers.

Pyridylamidohafnium catalysts are active for the high-temperature production of high-MW *i*PP (*17*) and chain-shuttling polymerization (*18*). We recently described the optimization of a pyridylamidohafnium catalyst (**1**) for the controlled isoselective polymerization of propylene (*19*). We report the use of the catalyst to produce high-MW *i*PP-*b*-PE diblock and multiblock copolymers with precise control of block length (Fig. 1).

The activation of precatalyst **1** with $B(C_6F_5)_3$, followed by the condensation of propylene into the reaction, afforded isotactic polypropylene (Fig. 1). After complete consumption of propylene, the introduction of ethylene to the reaction vessel resulted in the formation of a *i*PP-*b*-PE diblock copolymer. M_n values increased linearly as a function of monomer conversion and were in good agreement with theoretical values, consistent with the behavior of a living polymerization (*20*).

The MW of the ethylene block was controlled by varying reaction time (Table 1, entries 1 and 2)

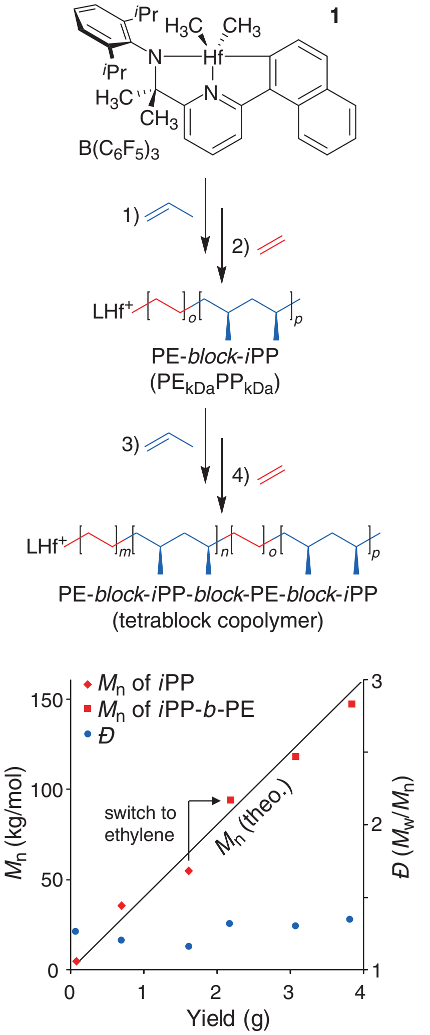

Fig. 1. Synthesis of PE/*i*PP block copolymers. The structure of isoselective pyridylamidohafnium catalyst (**1**)/$B(C_6F_5)_3$ and the controlled polymerization of olefins to ethylene and propylene multiblock copolymers are shown. After quenching with methanol, hafnium end groups were protonated. Number-average molecular weights (M_n) and dispersities ($Đ$ = M_w/M_n) were determined using size-exclusion chromatography calibrated with polyethylene standards. M_w, weight-average molecular weight; theo., theoretical; ^{i}Pr, isopropyl.

---

[1] Department of Chemistry and Chemical Biology, Baker Laboratory, Cornell University, Ithaca, NY 14853, USA. [2] Department of Chemical Engineering and Materials Science, University of Minnesota, Minneapolis, MN 55455, USA.
*Present address: Dipartimento di Scienze Chimiche, Università di Napoli Federico II, Complesso Monte S. Angelo, Via Cintia, I-80126 Napoli, Italy. **†Corresponding author. Email: lapointe@cornell.edu (A.M.L.); bates001@umn.edu (F.S.B.); coates@cornell.edu (G.W.C.)**

under a constant ethylene feed, whereas propylene MWs were tuned by the monomer:catalyst ratio and full conversion. The single melting endotherms observed (fig. S2) are due to regio- and stereoerrors in the propylene block. These errors lower the T_m of the *i*PP homopolymers to 134°C (versus ~165°C for perfect *i*PP), which is very similar to the T_m of the PE block (135°C). This was confirmed by quantitative ^{13}C nuclear magnetic resonance (NMR) spectroscopy (fig. S1), which showed high stereoselectivity for 1,2-insertion of polypropylene (m^4 = 91%). Regioerrors previously observed with this class of catalysts were also detected (*17*). The NMR spectrum showed neither detectable vinylidene end groups, which would arise from β-hydride elimination, nor peaks consistent with random ethylene-*co*-propylene segments; this confirms that there is minimal tapering in the materials. Consistent with this reactivity, catalyst **1**/B(C_6F_5)$_3$ was capable of synthesizing PE/*i*PP tetrablock copolymers (Table 1, entries 4 and 5). Gel permeation chromatography analysis of aliquots taken after complete consumption of the monomers showed that MWs increased after each monomer addition and molar mass dispersities remained low (fig. S3), although some MW broadening was observed due to precipitation of the insoluble, semicrystalline polymer.

Owing to thermodynamic incompatibility, weak van der Waals interactions, and the accumulation of amorphous polymer at the junction between melt-molded laminates, most commercial grades of *i*PP and PE homopolymers display poor interfacial adhesion (*9*). We used a simple peel test to evaluate adhesion between heterogeneous-grade PE and *i*PP laminates with and without the presence of the block copolymer as an adhesive layer (Fig. 2). Rectangular plaques of two (PE/*i*PP) and three layers (with block copolymer film) were compression-molded in the melt and then pulled apart while peel strength (S = force/sample width) was monitored. This test provided a facile method for comparing the interfacial strength between the molded films. We report the results obtained from 100-µm-thick block copolymer films, but note that no thickness dependence was observed down to 5-µm solvent cast films (fig. S9).

Figure 2 shows representative peel test results obtained as a function of block copolymer molecular architecture and MW. Laminates without block copolymers peel apart easily (S < 0.5 N/mm). Incorporation of the $PP_{24}PE_{31}$ and $PP_{73}PE_{50}$ diblock copolymers increases the peel strength to $S \approx$ 1 and 3 N/mm, respectively. Increasing the MW of both blocks beyond a threshold value leads to a substantial change in the failure mechanism from adhesive failure (low MWs) to cohesive failure (fracture, S > 6 N/mm) of the PE homopolymer film above ~75 kg/mol, as shown in Fig. 2 (see also figs. S4 and S5). The interfacial strength between the diblock and homopolymer films is dependent on the block sizes due to two factors. First, the block copolymer acts as a surfactant, eliminating the thermodynamic driving force for amorphous materials to localize at the interface between block copolymer and *i*PP and PE film junctions (*9*). In some respects, the block copolymer acts as a type of macromolecular welding flux material. Second, increasing the overall block size enhances interpenetration and the number of entanglements between the chemically identical blocks and homopolymer chains in the melt state (*21*, *22*). Moreover, we anticipate a threshold MW beyond which the polymer block will be able to bridge the amorphous layers associated with the

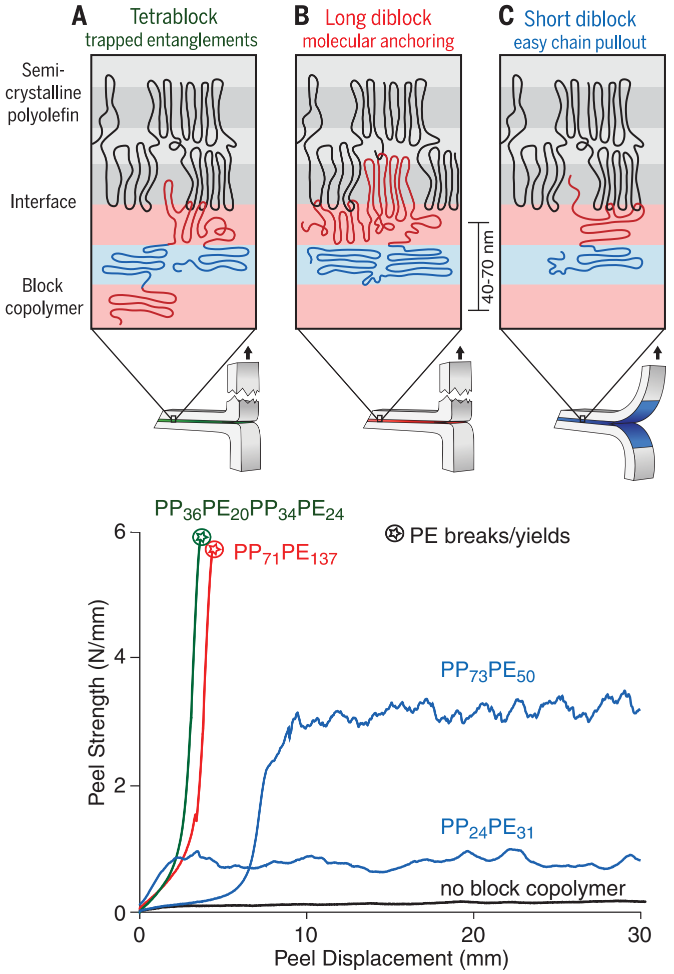

Fig. 2. Peel strength of commercial PE/*i*PP with various block copolymers. Rectangular sheets (0.6 cm by 6 cm, 340 µm thick) of PE/*i*PP were laminated in the melt at 180°C, with and without PE/*i*PP block copolymer layers (100 µm thick), and were pulled apart at 10 mm/min. After testing, specimens were investigated with scanning electron microscopy (fig. S6). Proposed models to explain the adhesive differences between (**A**) tetrablock, (**B**) high-M_n diblock, and (**C**) low-M_n diblock copolymers are shown. Block copolymers are in multiple lamellae (40 to 70 nm) (fig. S17); the first layer is shown. Stars indicate that PE films break or deform rather than undergo delamination.

Table 1. Properties of PE/*i*PP block copolymers. Cat., catalyst; $P_{ethylene}$, pressure of ethylene; t_{rxn}, reaction time; M_n, number-average molecular weight; *theo.*, theoretical; *tot.*, total; M_w, weight-average molecular weight; *Đ*, dispersity; T_m, melting temperature. See supplementary materials for experimental details.

Entry	Product ($PP_{kDa}PE_{kDa}$)	Cat. (µmol)	C_3H_6 (g)	$P_{ethylene}$ (atm)	t_{rxn} C_2H_4 (min)	Yield (g)	M_n (*theo.*) (kg/mol)	M_n (*tot.*) (kg/mol)	*Đ* (M_w/M_n)	T_m (°C)
1	$PP_{71}PE_{137}$	30	2.3	2.7	10	6.2	207	208	1.29	133
2	$PP_{73}PE_{50}$	30	2.3	2.7	5	3.9	130	123	1.29	131
3	$PP_{24}PE_{31}$	75	1.5	2.0	3	3.3	44	55	1.32	132
4	$PP_{36}PE_{20}PP_{34}PE_{24}$	25	1.0, 1.0	1.4, 1.4	4, 4	3.0	120	113	1.38	124
5	$PP_{60}PE_{80}PP_{75}PE_{90}$	30	2.0, 2.0	2.7, 2.7	4, 4	8.5	283	306	1.29	126

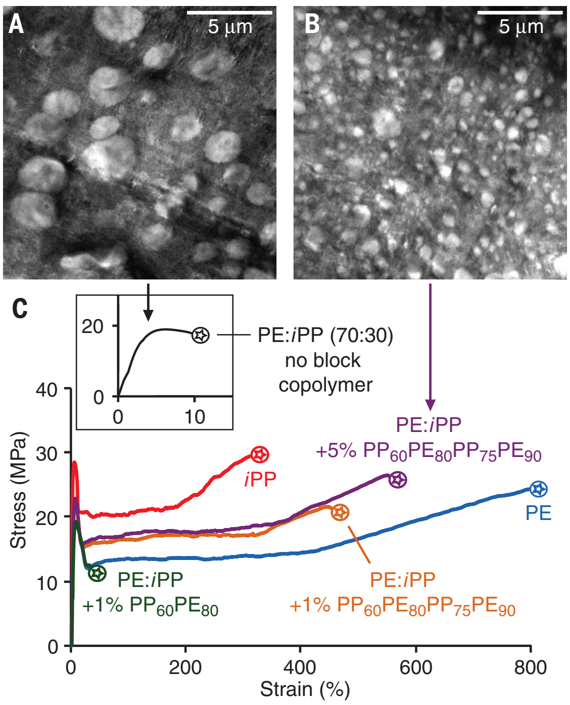

Fig. 3. Uniaxial tensile elongation of PE/*i*PP materials and blends. (**A** and **B**) Transmission electron microscopy images of PE/*i*PP blends show droplet morphology, both without block copolymers (A) and with 5 wt % tetrablock copolymers (B). (**C**) Materials were melt-blended at 190°C without block copolymers (black) or with 1 wt % diblock (green), 1 wt % tetrablock (orange), or 5 wt % tetrablock copolymers (purple). These materials were then compression molded into tensile specimens at 180°C and strained at a rate of 100%/min (fig. S10).

lamellar morphology of semicrystalline polymers such as *i*PP and PE, leading to cocrystallization along the film interfaces, as shown in Fig. 2B and fig. S15 (*21*). Lower-MW blocks are less capable of reaching the homopolymers' crystalline lamellae (Fig. 2C) and will be prone to chain pullout, resulting in lower adhesive strength. The welding effect was observed in various polyolefin materials (fig. S7) and only with semicrystalline block polymer adhesives (fig. S8).

The $PP_{36}PE_{20}PP_{34}PE_{24}$ tetrablock copolymer exhibits considerable adhesive strength evidenced by cohesive failure (Fig. 2A), which seemingly contradicts the aforementioned arguments, as all of the blocks are well below the threshold MW required for cohesive failure with diblocks. Thus, we invoke a different mechanism for this result. A tetrablock molecular architecture ensures that half of the *i*PP and PE blocks are flanked by thermodynamically incompatible counterparts. This implies that interfacial mixing during melt compression produces entangled loops that effectively stitch together the homopolymers and block copolymer films upon crystallization when the laminates are cooled, as illustrated in Fig. 2A. Similar arguments account for the enhanced toughness of bulk multiblock versus triblock polymers (*23*, *24*). Consistent with this line of reasoning, the $PP_{36}PE_{20}PP_{34}PE_{24}$ tetrablock copolymer is microphase-separated up to 260°C, as shown by rheological measurements (fig. S17).

Challenges of recycling mixed polyolefin municipal waste (typically 70:30 PE:*i*PP) are partly due to phase separation and fragile interfaces, which results in poor mechanical properties (*5*–*7*). Because specialty grades of PE and *i*PP can be blended to improve impact and crack resistance, the effective compatibilization of heterogeneous-grade polyolefins may allow an upcycling of plastic wastes into higher-value materials (*12*). Figure 3A shows the morphology obtained from a heterogeneous-grade polyolefin blend containing 70 weight % (wt %) PE and 30 wt % *i*PP, and Fig. 3B illustrates the consequences of adding 5 wt % tetrablock $PP_{60}PE_{80}PP_{75}PE_{90}$ to this mixture. Interfacial activity of the block copolymer is evidenced by a reduction in the average droplet size from 2.2 to 0.55 μm with the addition of the tetrablock copolymer; similar results were obtained with other architectures (figs. S11 to S14).

Individually, pure *i*PP and PE display ductility and strain hardening when pulled in tension at room temperature (Fig. 3C). Blending the two components leads to a phase-separated material and a marked reduction in strain at the break point (ε_b = 12% versus 300 and 800% for *i*PP and PE, respectively). The addition of 5 wt % $PP_{60}PE_{80}PP_{75}PE_{90}$ raises ε_b to 600%, owing to the combined effects of interfacial adhesion, reduced particle size, and efficient stress transfer between phases (fig. S16). With just 1% of this tetrablock copolymer, ε_b = 450%, whereas the addition of 1 wt % of the corresponding diblock copolymer ($PP_{60}PE_{80}$) leads to a modest improvement (ε_b = 90%). The low-MW tetrablock polymer $PP_{36}PE_{20}PP_{34}PE_{24}$ exhibited similar properties, as did other blends with different PE:*i*PP ratios (fig. S18).

We have developed a catalyst system capable of synthesizing semicrystalline PE/*i*PP multiblock copolymers with precise control over block length and architecture. These macromolecules form strong interfaces with commercial PE and *i*PP when properly designed. Two molecular mechanisms are proposed to explain the MW dependence of diblock copolymer adhesion and the behavior of tetrablock copolymers with relatively short blocks. The interfacial strength translates into control over morphology and mechanical toughness in melt blends of commercial PE and *i*PP, blends that are otherwise brittle at a ratio typically found in municipal waste streams.

REFERENCES AND NOTES

1. D. B. Malpass, E. I. Band, "Introduction to polymers of propylene," in *Introduction to Industrial Polypropylene: Properties, Catalysis, Processes* (Scrivener, 2012), pp. 1–18.
2. M. Stürzel, S. Mihan, R. Mülhaupt, *Chem. Rev.* **116**, 1398–1433 (2016).
3. W. Kaminsky, Ed., *Polyolefins: 50 Years After Ziegler and Natta I* (Advances in Polymer Science Series, Springer, 2013).
4. D. Nwabunma, T. Kyu, Eds., *Polyolefin Blends* (Wiley, 2008).
5. "The new plastics economy: Rethinking the future of plastics" (Ellen MacArthur Foundation, 2016); www.ellenmacarthurfoundation.org/publications/the-new-plastics-economy-rethinking-the-future-of-plastics.
6. M. Chanda, S. K. Roy, Eds., in *Plastics Fabrication and Recycling* (Plastics Engineering Series, Taylor and Francis, 2009), pp. 2-1–2-41.
7. M. Xanthos, *Science* **337**, 700–702 (2012).
8. L. Resconi, L. Cavallo, A. Fait, F. Piemontesi, *Chem. Rev.* **100**, 1253–1346 (2000).
9. K. A. Chaffin, J. S. Knutsen, P. Brant, F. S. Bates, *Science* **288**, 2187–2190 (2000).
10. G. J. Domski, J. M. Rose, G. W. Coates, A. D. Bolig, M. Brookhart, *Prog. Polym. Sci.* **32**, 30–92 (2007).
11. P. D. Hustad, *Science* **325**, 704–707 (2009).
12. J. W. Teh, A. Rudin, J. C. Keung, *Adv. Polym. Technol.* **13**, 1–23 (1994).
13. Y. Lin, V. Yakovleva, H. Chen, A. Hiltner, E. Baer, *J. Appl. Polym. Sci.* **113**, 1945–1952 (2009).
14. A. Colbeaux, F. Fenouillot, J.-F. Gérard, M. Taha, H. Wautier, *J. Appl. Polym. Sci.* **95**, 312–320 (2005).
15. V. Busico, R. Cipullo, N. Friederichs, S. Ronca, M. Togrou, *Macromolecules* **36**, 3806–3808 (2003).
16. V. Busico *et al.*, *Macromolecules* **37**, 8201–8203 (2004).
17. T. R. Boussie *et al.*, *Angew. Chem. Int. Ed.* **45**, 3278–3283 (2006).
18. D. J. Arriola, E. M. Carnahan, P. D. Hustad, R. L. Kuhlman, T. T. Wenzel, *Science* **312**, 714–719 (2006).
19. G. W. Coates, G. J. Domski, Patent WO 2008112133A2 (2008).
20. O. W. Webster, *Science* **251**, 887–893 (1991).
21. J. J. Benkoski, P. Flores, E. J. Kramer, *Macromolecules* **36**, 3289–3302 (2003).
22. C. Laurens, C. Creton, L. Léger, *Macromolecules* **37**, 6814–6822 (2004).
23. A. Phatak, L. S. Lim, C. K. Reaves, F. S. Bates, *Macromolecules* **39**, 6221–6228 (2006).
24. F. S. Bates *et al.*, *Science* **336**, 434–440 (2012).

ACKNOWLEDGMENTS

Financial support for this work was provided by the Center for Sustainable Polymers, an NSF Center for Chemical Innovation (grant CHE-1413862). The Cariplo Foundation ("Crystalline Elastomers Project") provided funding to R.D.G. We thank N. Chen, S. Hayrapetyan, and M. Silberstein for assistance with melt-blend and tensile studies and I. Keresztes for assistance with NMR spectroscopy. J.M.E., A.M.L., and G.W.C. are inventors on U.S. patent applications 62/421,680 and 62/342,583, submitted by Cornell University, which cover welds and compatibilization of polyolefin materials. All data are available in the supplementary materials. Author contributions: G.W.C. conceived the project. G.W.C., J.M.E., R.D.G., and A.M.L. designed and conducted experiments related to polymer synthesis. J.M.E., J.X., and C.M.T. designed and conducted experiments related to adhesion and blends. G.W.C., A.M.L., C.W.M., and F.S.B. designed experiments and directed research. J.M.E., G.W.C., A.M.L., J.X., and F.S.B. wrote the manuscript. All authors commented on the manuscript.

SUPPLEMENTARY MATERIALS

www.sciencemag.org/content/355/6327/814/suppl/DC1
Materials and Methods
Figs. S1 to S18
References (*25*–*27*)

1 September 2016; accepted 25 January 2017
10.1126/science.aah5744

Combining polyethylene and polypropylene: Enhanced performance with PE/ *i*PP multiblock polymers

James M. Eagan, Jun Xu, Rocco Di Girolamo, Christopher M. Thurber, Christopher W. Macosko, Anne M. LaPointe, Frank S. Bates and Geoffrey W. Coates (February 23, 2017)

Science **355** (6327), 814-816. [doi: 10.1126/science.aah5744]

Editor's Summary

How to make opposites compatible

Polyethylene (PE) and isotactic polypropylene (*i*PP) are the two most widely used commodity plastics and thus make up a large fraction of the waste stream. However, the two plastics will not mix together, which limits options for dealing with mixed waste and decreases the value of recycled products. Eagan *et al.* report the synthesis of multiblock copolymers of *i*PP and PE by using a selective polymer initiator (see the Perspective by Creton). The high-molecular-weight blocks could be used to reinforce the interface between *i*PP and PE and allow blending of the two polymers.

Science, this issue p. 814; see also p. 797

Science (print ISSN 0036-8075; online ISSN 1095-9203) is published weekly, except the last week in December, by the American Association for the Advancement of Science, 1200 New York Avenue NW, Washington, DC 20005.